
VIII.

The Sky Seen in γ -rays

Astroparticle Physics a.a. 2021/22

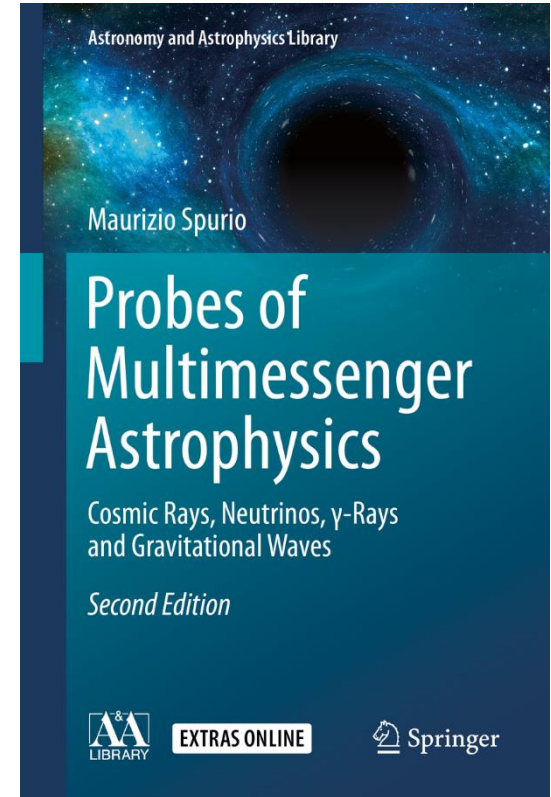
Maurizio Spurio

Università di Bologna e INFN

maurizio.spurio@unibo.it

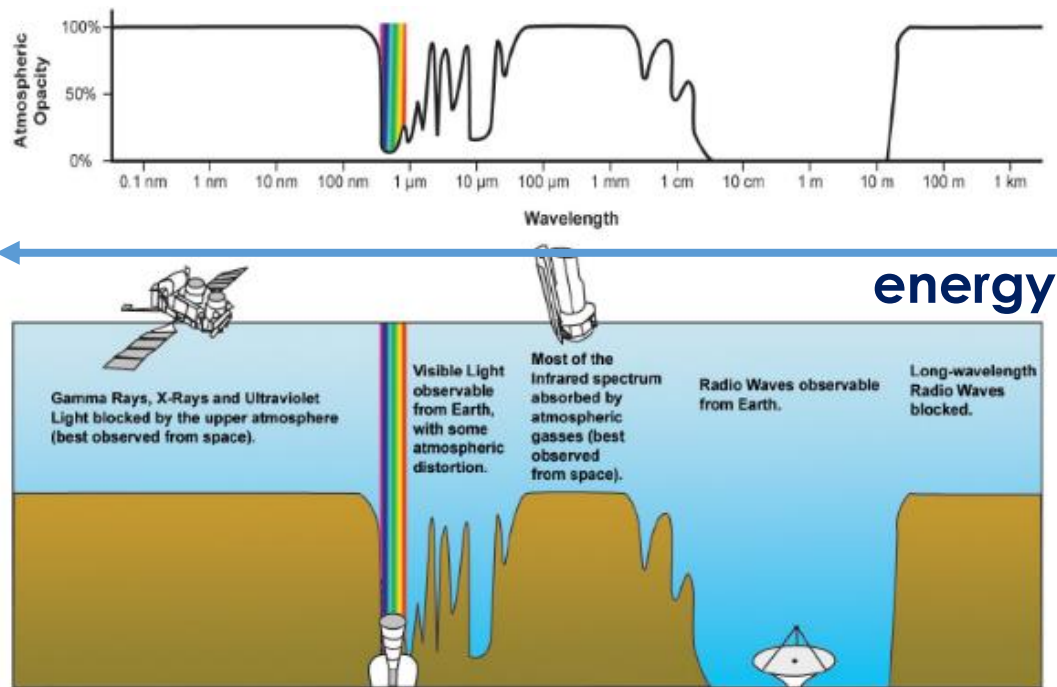
Content

8	The Sky Seen in γ-rays
8.1	The Spectral Energy Distribution (SED) and Multiwavelength Observations
8.2	Astrophysical γ -rays: The Leptonic Model
8.2.1	The Synchrotron Radiation from a Power-Law Spectrum ..
8.2.2	Synchrotron Self-Absorption
8.2.3	Inverse Compton Scattering
8.3	The Synchrotron Self-Compton (SSC) Mechanism
8.4	Astrophysical γ -rays: The Hadronic Model
8.5	Energy Spectrum of γ -rays from π^0 Decay
8.6	Galactic Sources and γ -rays: A Simple Estimate
8.7	The Compton Gamma-Ray Observatory (CGRO) Legacy
8.7.1	The EGRET γ -ray Sky
8.8	Fermi-LAT and Other Experiments for γ -ray Astronomy
8.8.1	The Fermi-LAT
8.8.2	The Fermi-GBM
8.8.3	AGILE
8.8.4	Swift
8.9	Diffuse γ -rays in the Galactic Plane
8.9.1	An Estimate of the Diffuse γ -ray Flux
8.10	The Fermi-LAT Catalogs
8.11	Gamma Ray Bursts
8.12	Classification of GRBs
8.13	Limits of γ -ray Observations from Space
	References

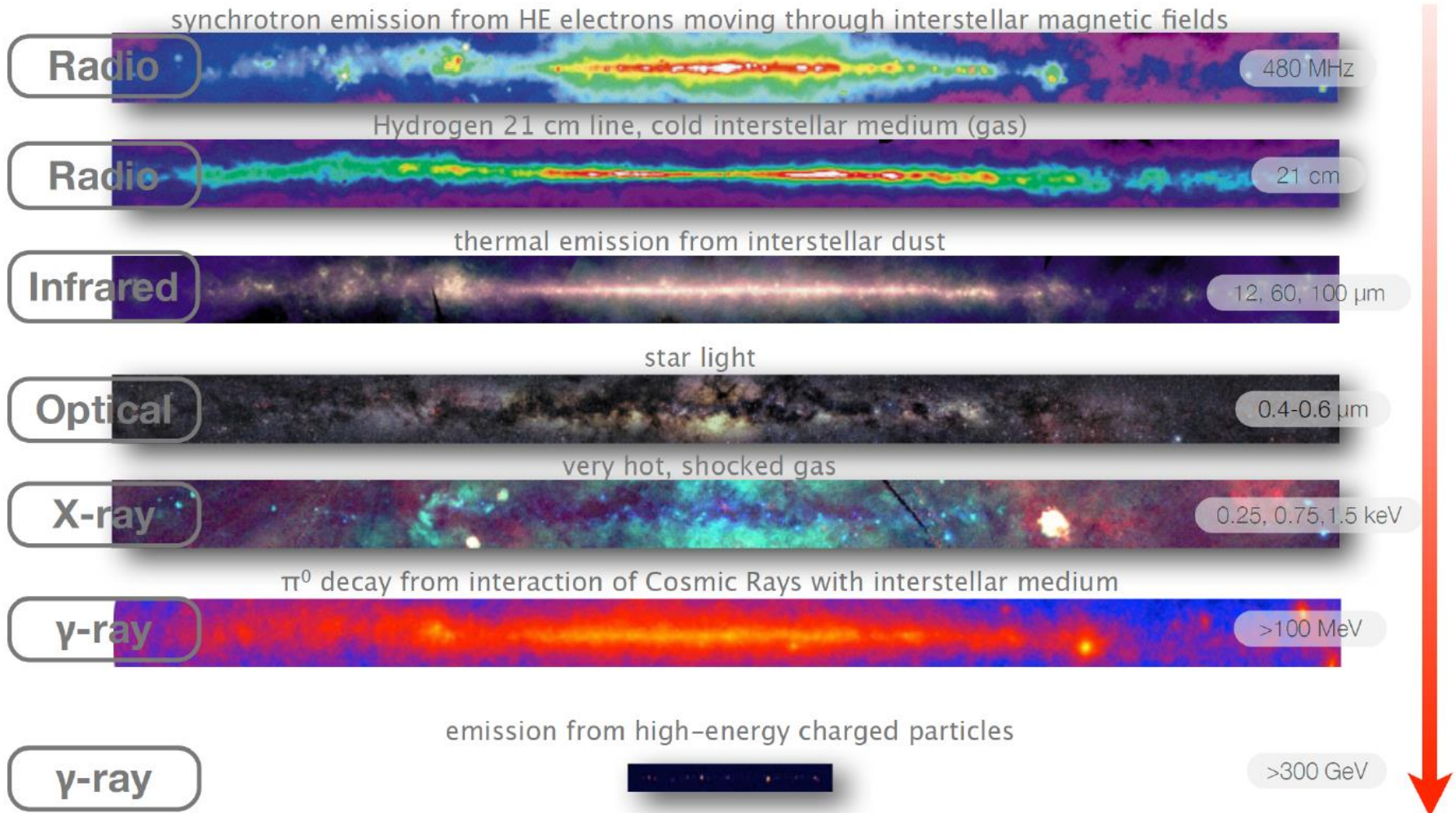


Introduction to γ -ray astronomy

- The presence of magnetic fields makes it (almost) impossible to localize CR sources using charged particles.
- The only way to gain information about their acceleration sites is by observing the neutral particles (γ -rays and neutrinos) generated by CR interactions at sources
- Recently, a new window has been opened on the observation of γ -rays up to the highest energies. The development has been made possible by the availability of new detectors coming from technologies typical of experimental particle physics.
- Space experiments cover the energy region from MeV to hundreds of GeV.
- Beyond a few hundreds GeV, the γ -ray fluxes are so small that space-based experiments cannot provide adequate statistics.
- Studies of at the $>TeV$ energies rely on ground-based detectors.

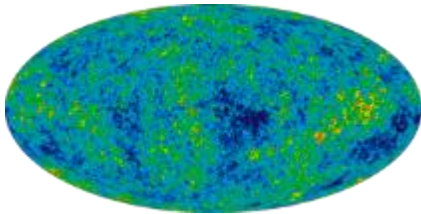
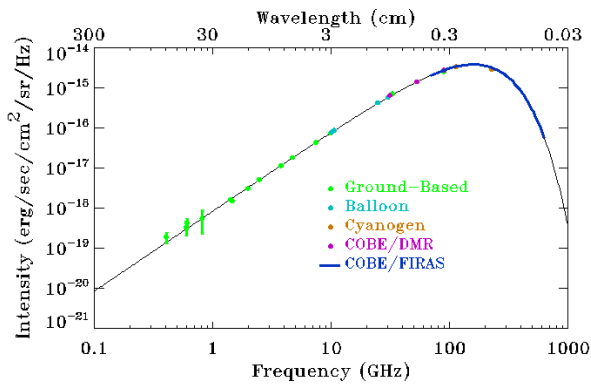


«Traditional» Astronomy



The Thermal Universe: the black-body spectrum

CMBR: 2.7 K

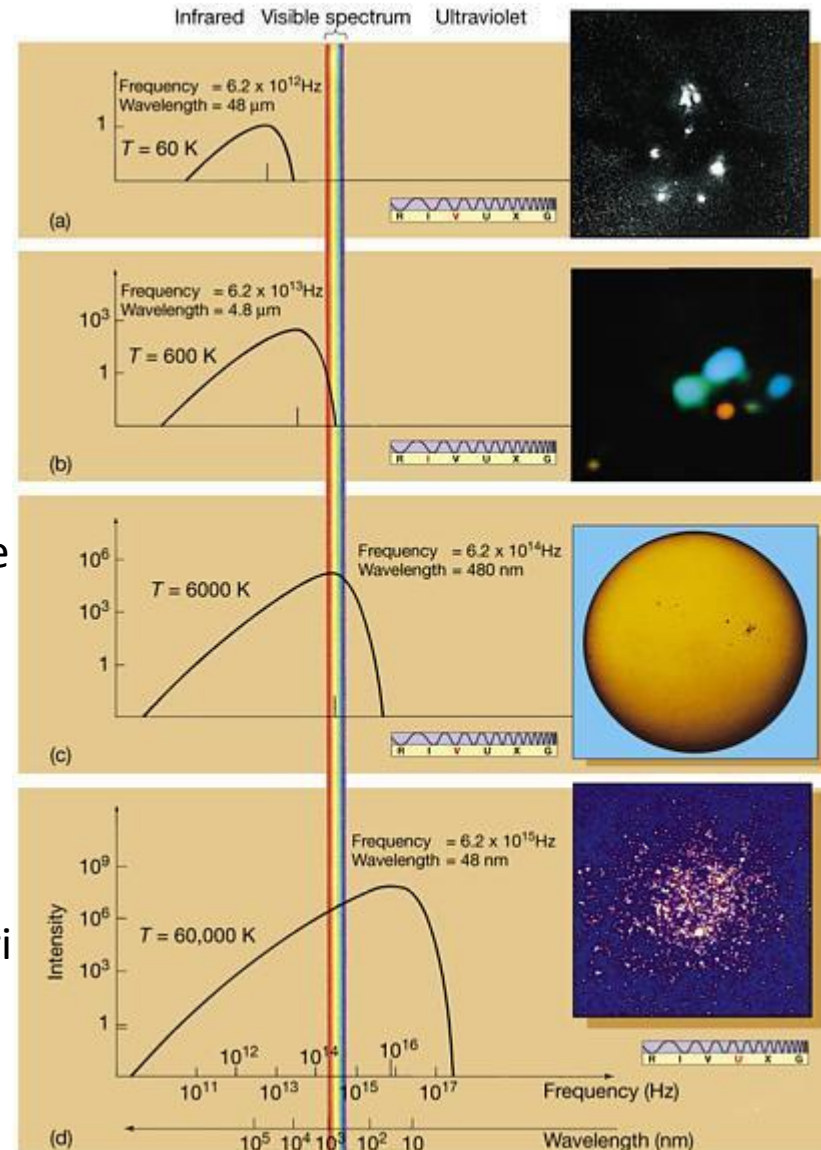


A Galactic gas cloud: 60 K

Star in the Orion Nebula: 600 K

The Sun surface 6000 K

Cluster of very bright stars, Omega Centauri 60,000 K

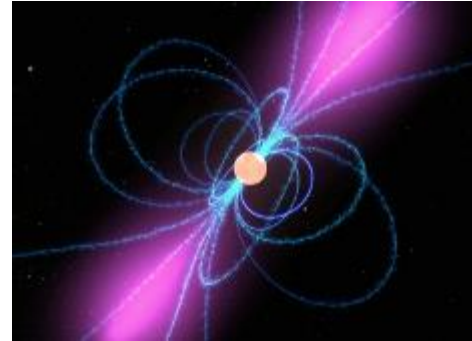


Examples of non-thermal environments

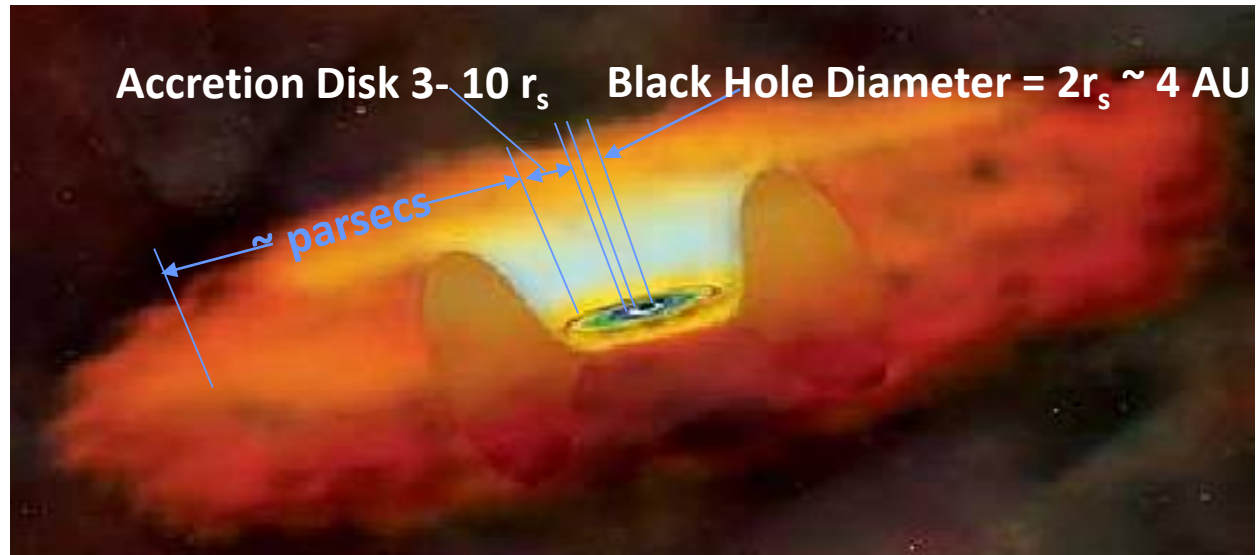
GRB



SuperNova Remnants
Pulsars

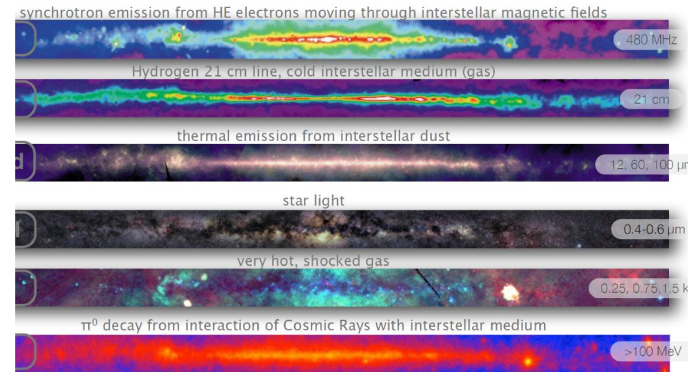
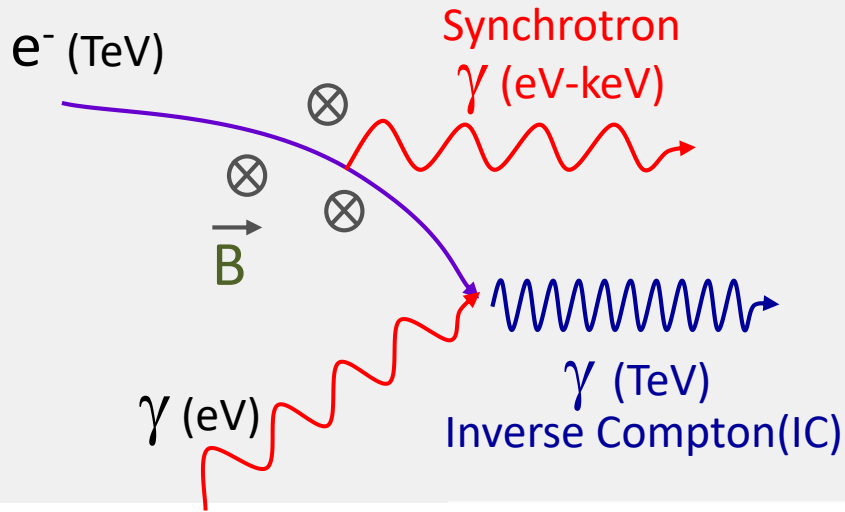


Active Galactic Nuclei

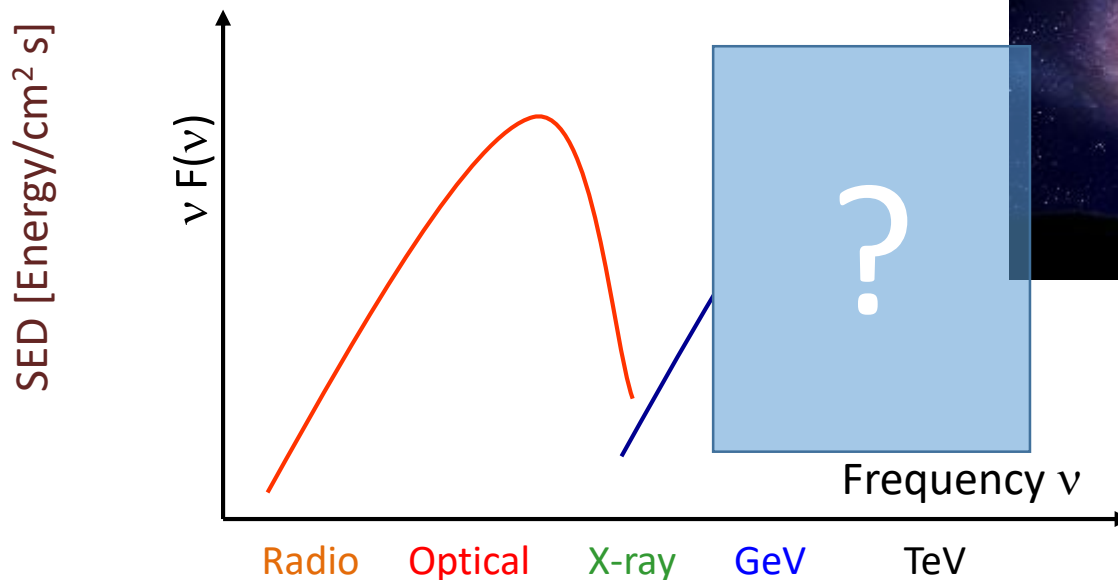


Non-thermal Universe: leptonic model

leptonic processes

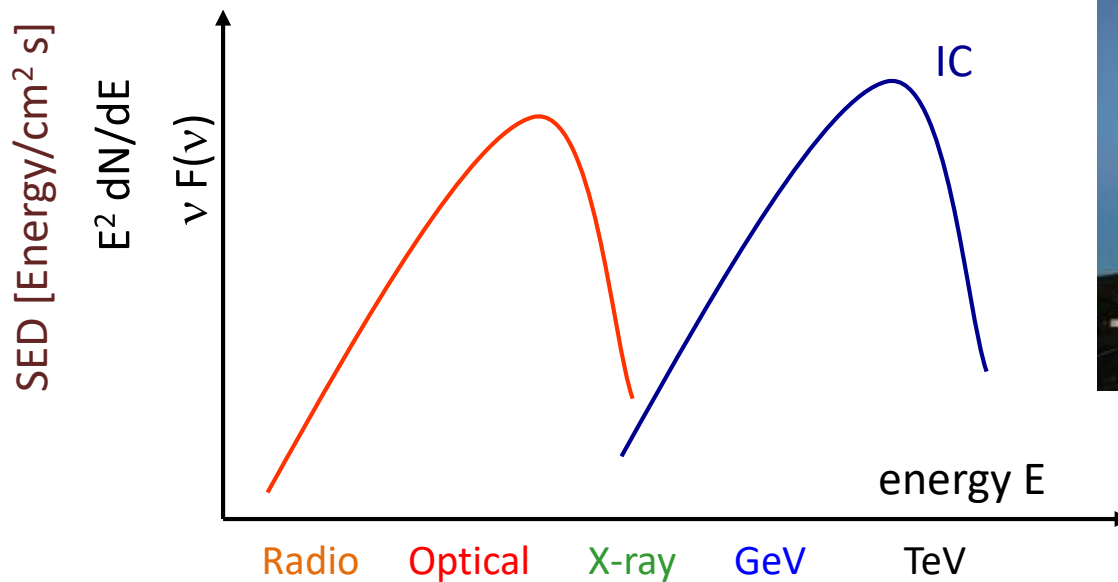
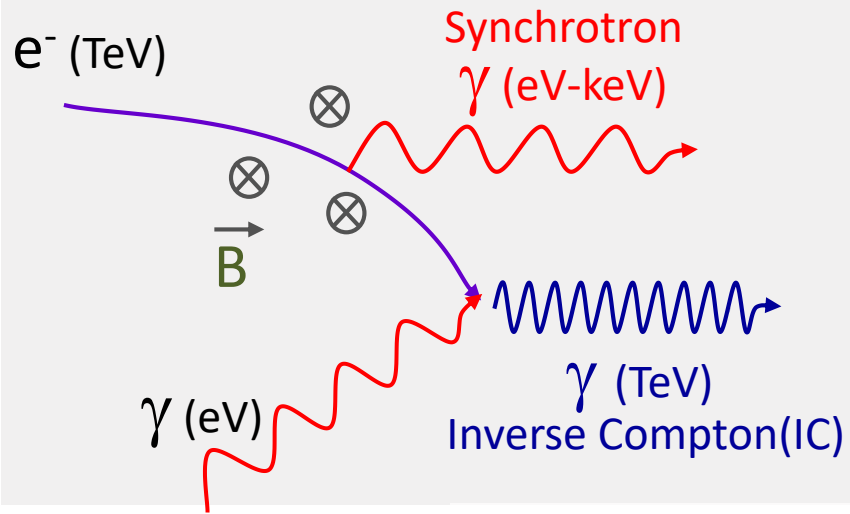


Traditional Astronomy



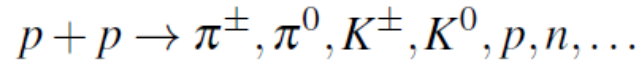
Non-thermal Universe: leptonic model

leptonic processes

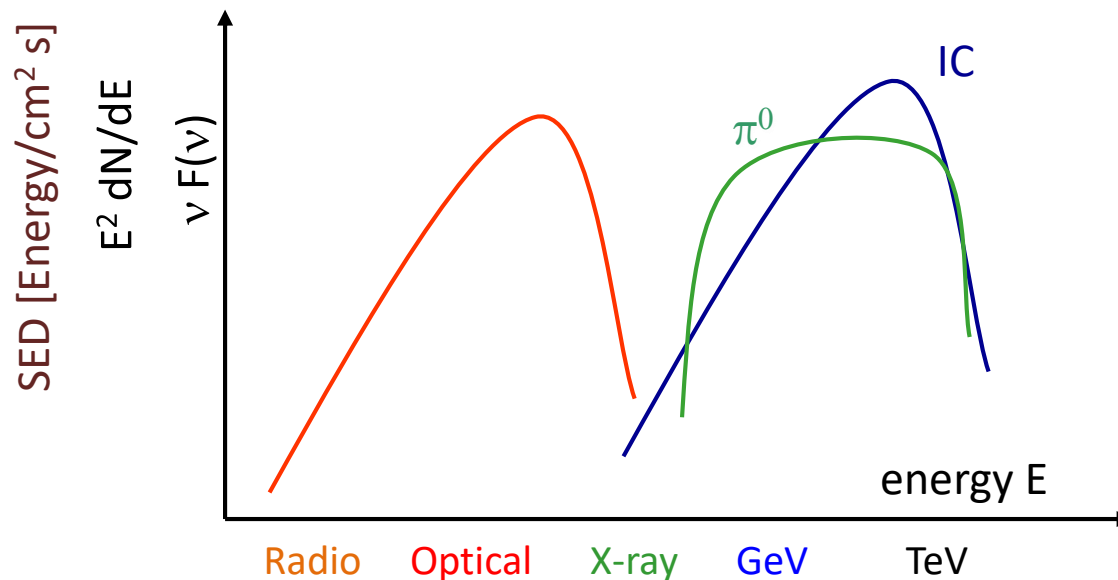
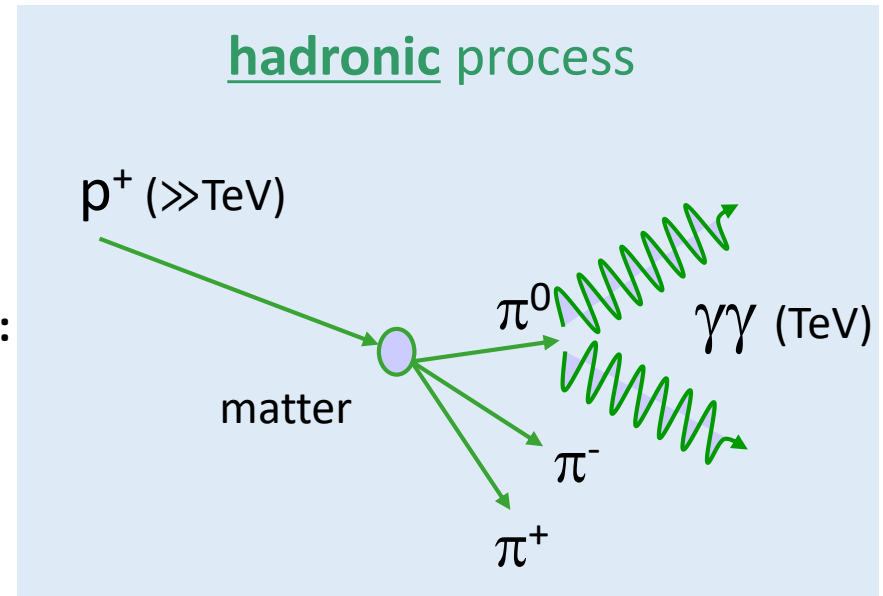
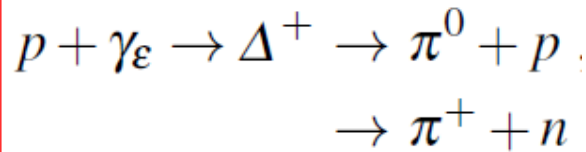


Non-thermal Universe: hadronic model

1) Astrophysical beam dump mechanism.

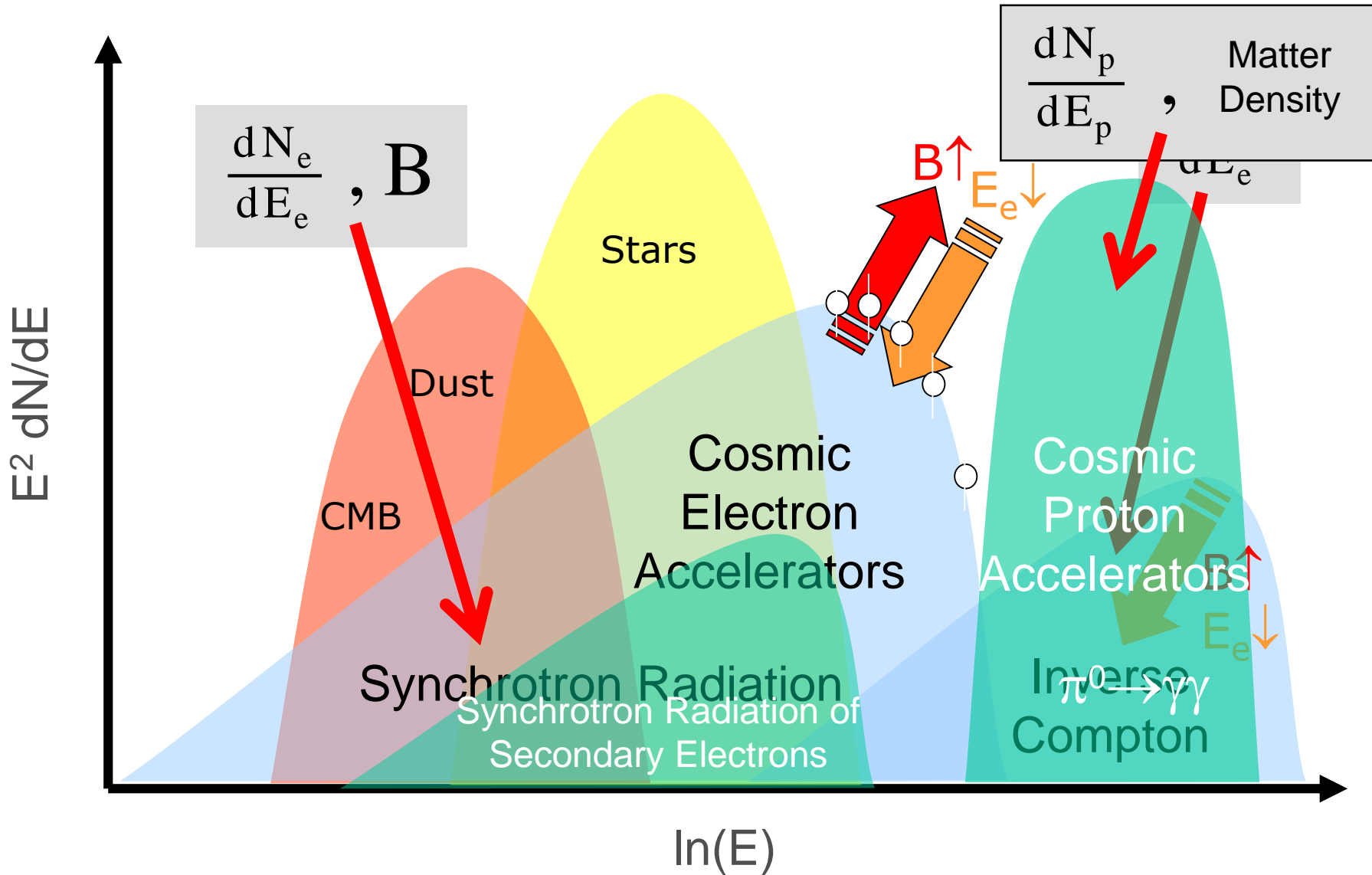


2) Photoproduction through the Δ^+ resonance:



To distinguish between **hadronic/leptonic** origin the **Spectral Energy Distribution (SED)** must be studied with different experimental techniques.

The Spectral Energy Distribution (SED)



Compton Gamma Ray Observatory (CGRO)

- Second NASA telescope mission after Hubble. Launched using the Space Shuttle in April 1991 and operated successfully until it was de-orbited on June 4, 2000
- The CGRO carried **four** instruments for γ -ray astronomy, each with its own energy range, detection technique, and scientific goals, covering energies from less than 15 keV to more than 30 GeV

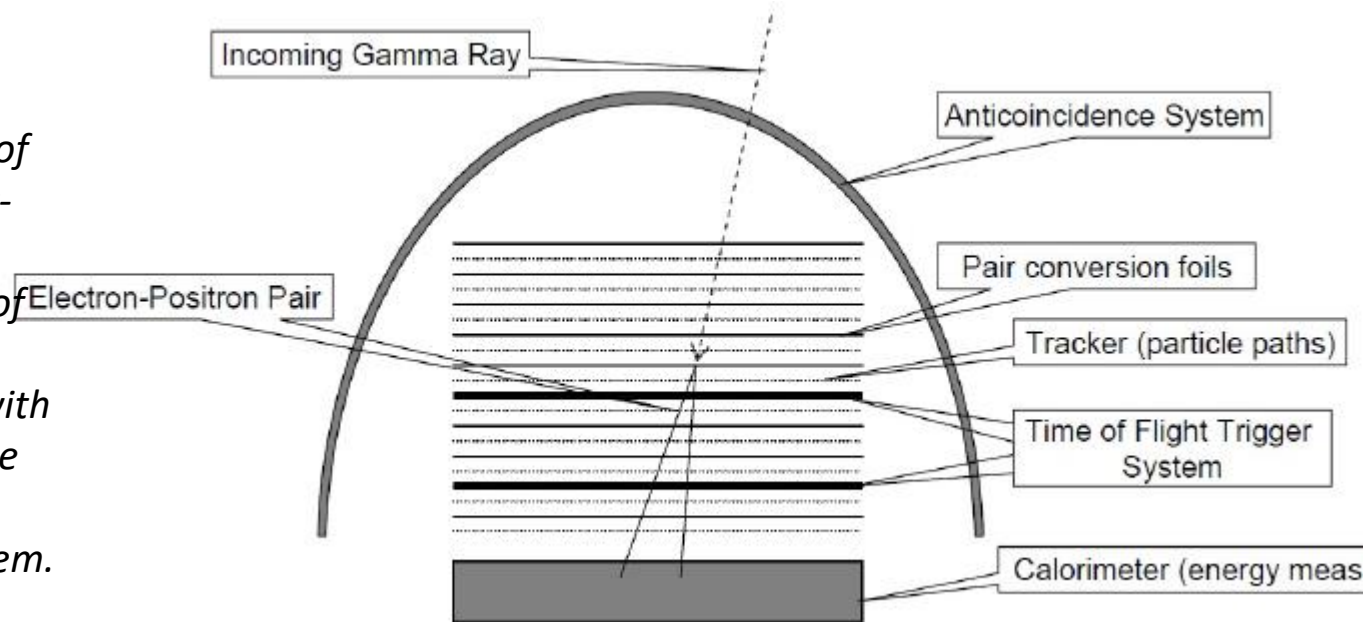
1. The Burst and Transient Source Experiment (**BATSE**) consisting of eight modules located one on each corner of the spacecraft. Each module was a large flat NaI(Tl) scintillator+a smaller thicker scintillator, combined to cover energies 15 keV -1 MeV.
2. Oriented Scintillation Spectrometer Experiment (**OSSE**). It used four large, collimated scintillator detectors to study γ -rays from 60 keV to 10 MeV.
3. The Compton Telescope (**COMPTEL**), for medium energy γ -rays between 0.8 MeV and 30 MeV: it used a Compton scattering technique.
4. The Energetic Gamma Ray Experiment Telescope (**EGRET**) was the high-energy instrument on CGRO, covering the energy range from 20 MeV to 30 GeV.



EGRET on CGRO

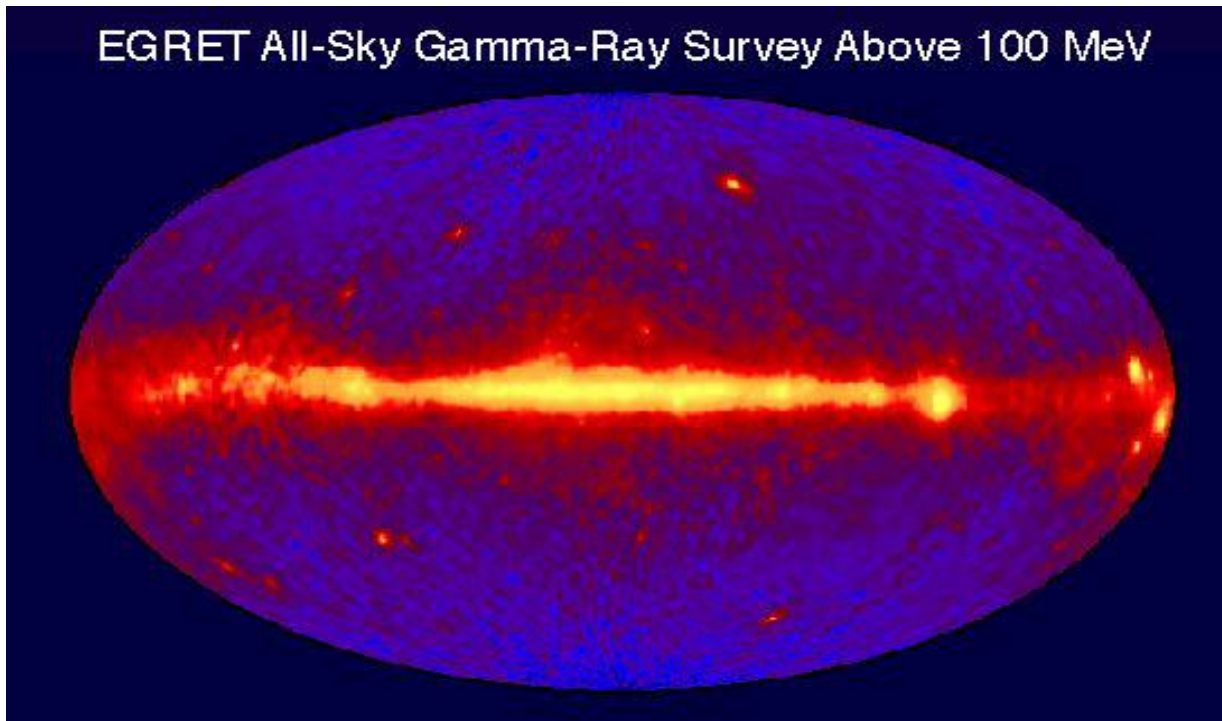
- Above 10 MeV, the principal interaction process for γ -rays is pair production.
- Gamma rays cannot be reflected or refracted, and a high-energy γ -ray telescope detects e^\pm with a precision converter-tracker section followed by a calorimeter.
- An external *veto* removes incoming charged particles (background)
- The two key challenges for any such telescope are:
 1. the identification of γ -ray interaction among the huge background of charged CRs;
 2. the measurement of γ -ray energy, arrival time and arrival direction.

- *Diagram of a telescope which use the conversion of a γ -ray into a e^\pm pair (pair-conversion telescope), reproducing the features of the EGRET experiment.*
- *The Fermi-LAT is similar, with an improved tracker device which avoids the use of a Time of Flight trigger system.*



The EGRET γ -ray sky (2000)

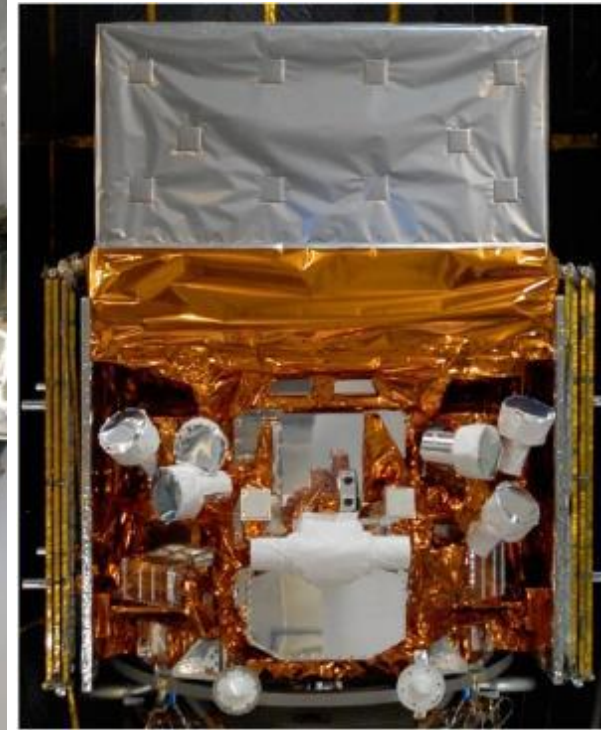
- A γ -ray source appears as an excess of photon counts above the diffuse emission
- A characteristic of the γ -ray sky is that it is highly variable,
- The last EGRET analysis produced the 3rd catalog containing 271 objects.
- The angular resolution cannot be compared with that reached in other wavelengths.
- Only 40% of the 271 γ -ray EGRET sources have been associated with known objects: the LMC, 94 blazars and 5 galactic pulsars. The remaining 170 sources had no identification



Fermi-LAT

“A revolution is underway in our understanding of the high energy sky”.

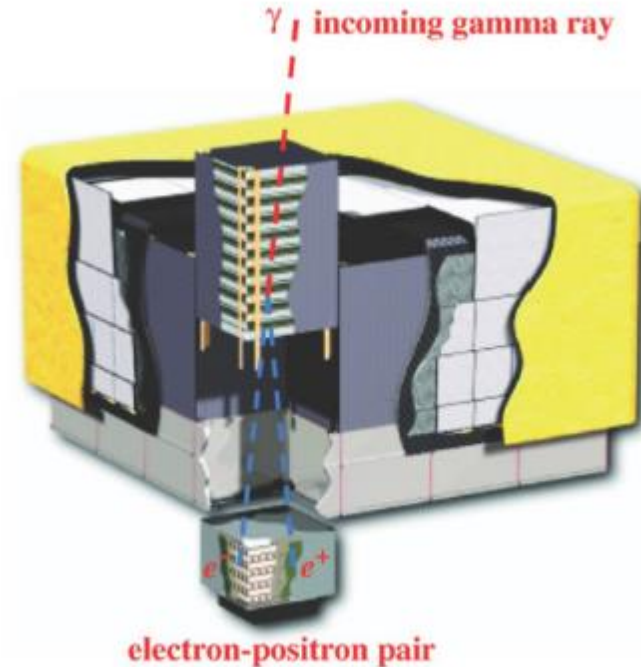
(The introductory sentence of the Fermi-LAT technical paper of 2009.)



Launch: June 11 2008

The FERMI-LAT detector

- The LAT is pair-conversion telescope with a precision converter-tracker and a calorimeter (a 4x4 array of 16 modules, Figure).
- The LAT's improved sensitivity w.r.t. EGRET is due to:
 - a large effective area ($\sim 8000 \text{ cm}^2$, $\sim 6 \times$ EGRET's);
 - large field of view ($\sim 2.4 \text{ sr}$, $\sim 5 \times$ EGRET's);
 - good background rejection;
 - superior angular resolution
 - No need of the ToF triggering system used in EGRET



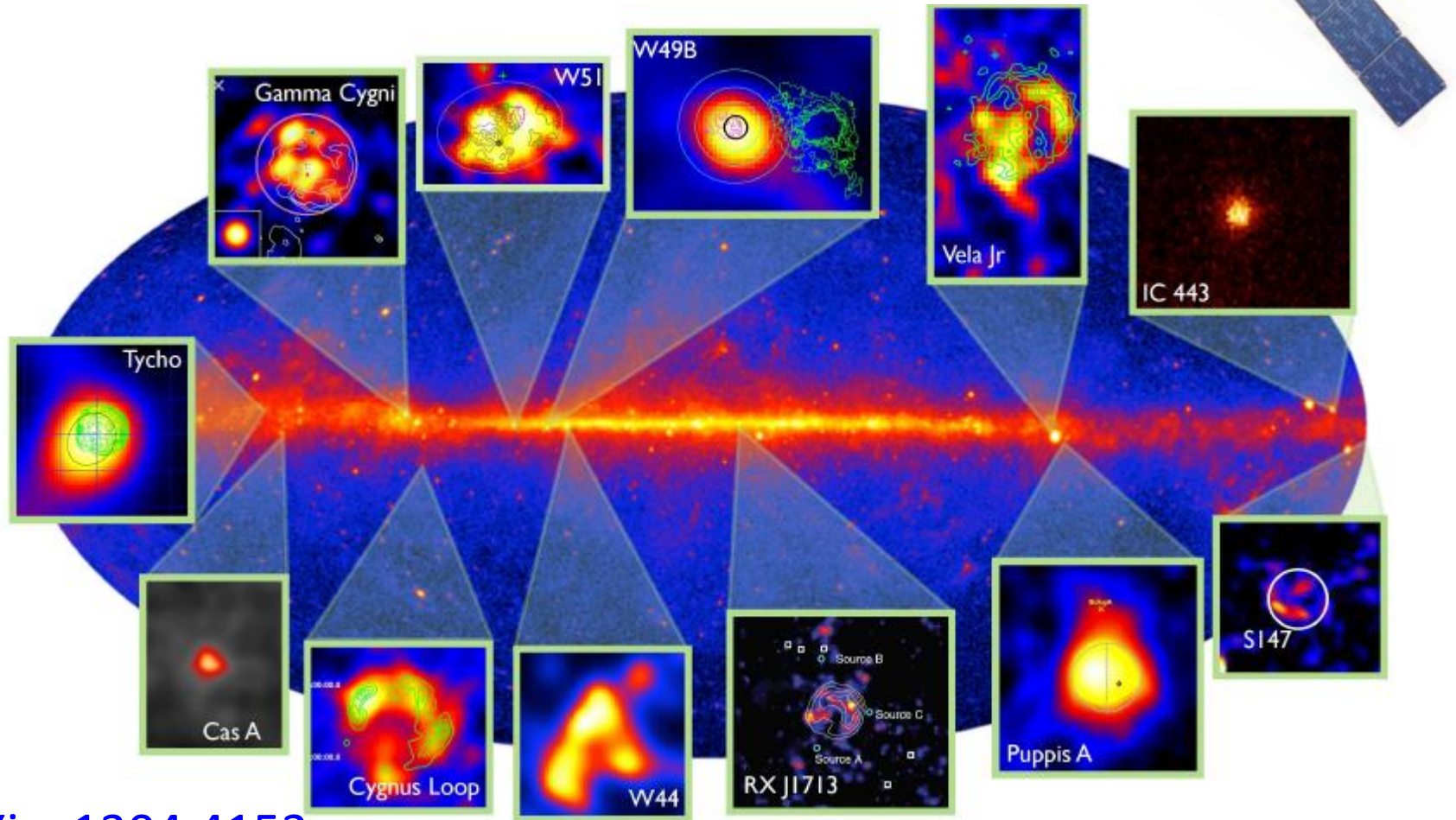
<http://fermi.gsfc.nasa.gov/>



- For each γ -ray, the arrival time, direction, and energy are measured.
- The angular resolution depends on E_γ : from 0.8° @ 1 GeV down to 0.2° @ 300 GeV.
- The observing efficiency is very high; LAT is off for 13% live time when it passes through regions where charged particles are trapped by the Earth's magnetic field .

The sky seen in the GeV range

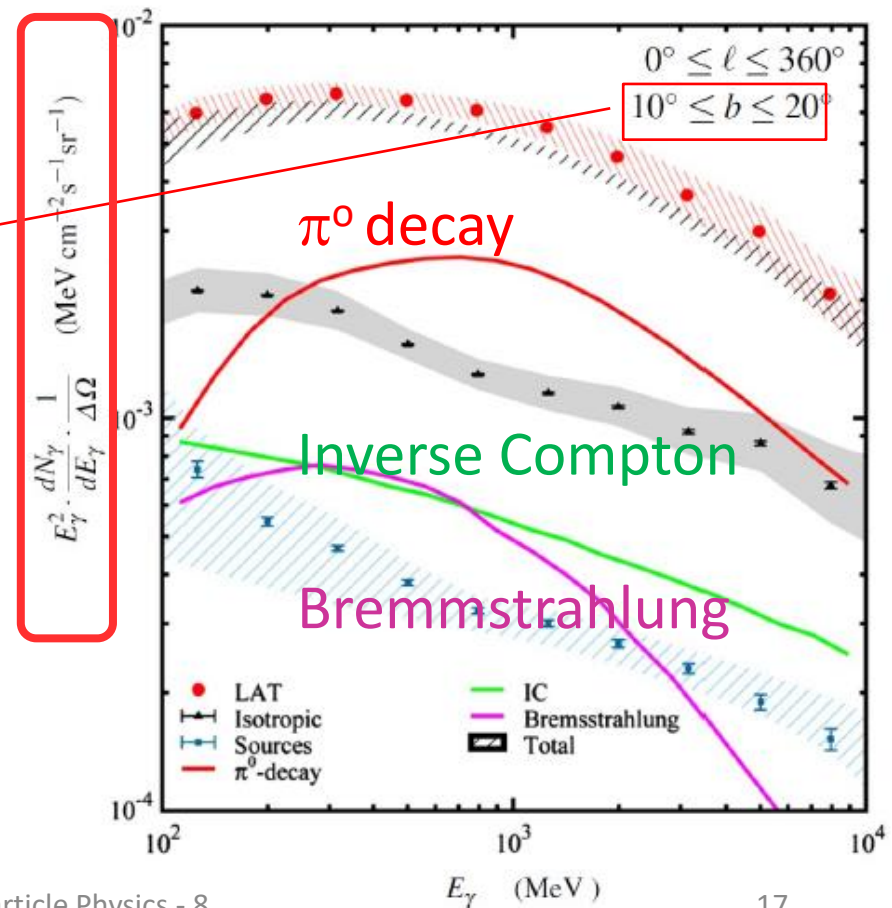
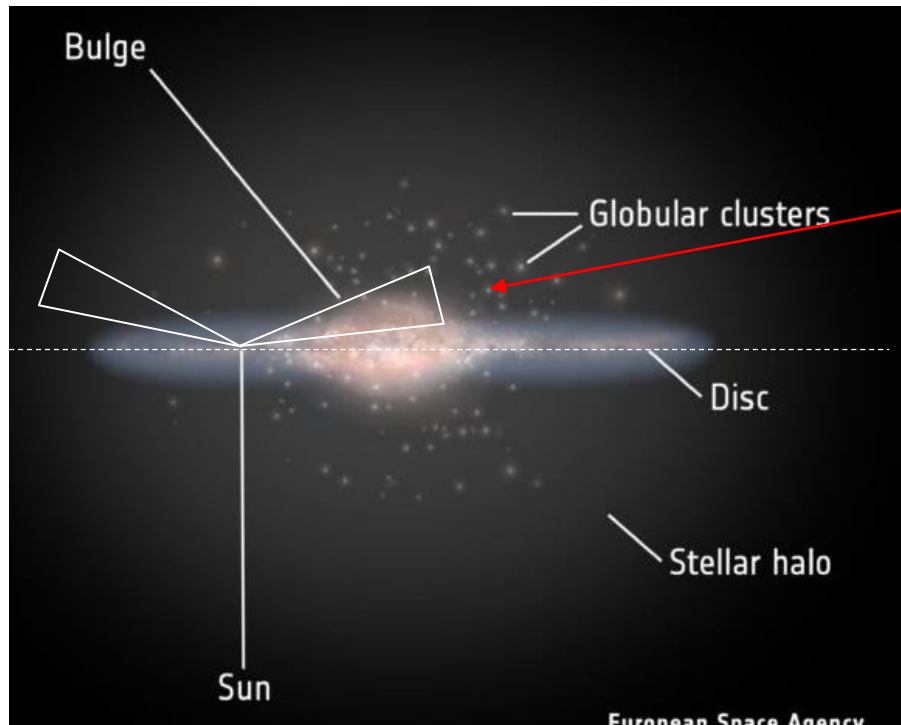
Diffuse + point sources



arXiv :1304.4153

The diffuse flux from the Galactic plane

- Unlike the sky at visible wavelengths, the γ -ray sky is dominated by a diffuse radiation originating in our Galaxy
- This diffuse γ -ray radiation is largely produced by galactic CRs interacting with the interstellar gas, demonstrating that CRs are permeating the whole Galaxy



FERMI LAT OBSERVATION OF DIFFUSE GAMMA RAYS PRODUCED THROUGH INTERACTIONS BETWEEN LOCAL INTERSTELLAR MATTER AND HIGH-ENERGY COSMIC RAYS

A. A. Abdo et al 2009 *ApJ* **703** 1240-1256 doi: [10.1088/0004-637X/703/2/1240](https://doi.org/10.1088/0004-637X/703/2/1240) [\(Help\)](#)

The diffuse flux from the Galactic plane

The processes that produce the observed γ -rays are due to:

- Inelastic collisions of CR with the interstellar gas during their propagation.
- CR electrons colliding with low-energy photons (Inverse Compton)
- High-energy electrons interacting with the gas, producing bremsstrahlung γ -rays

We can obtain an order of magnitude estimate using the following ingredients.

1. Cross-section. We assume that both CRs and target materials are protons, with inelastic cross-section: $\sigma_{pp} \simeq 40 \text{ mb} = 4 \cdot 10^{-26} \text{ cm}^2$
2. Number density of target material n (Chap. 2) : $n = n_{ISM} = 0.3 \text{ to } 1 \text{ cm}^{-3}$
3. Energy density, $\rho_{CR \rightarrow \gamma}$, of CRs producing the γ -rays observed by LAT corresponds to about 10% of the total energy density (threshold energy for the $pp \rightarrow pp\pi^0$ process)
4. Energy transferred, ΔE , to γ -rays in the process $pp \rightarrow \text{hadrons}$ depends on the energy E of the incoming proton ($\sim 10\%$ of E at threshold $pp \rightarrow pp\pi^0$, and rises to about $\sim 1/3$ at very high energies). As a rule of thumb, we assume $\Delta E/E = 1/6$.

Diffuse flux: a simple estimate

- The interaction rate of a relativistic CR with target protons of the ISM corresponds to

$$R_{\text{coll}} = \sigma_{pp} \cdot n \cdot c = 4 \cdot 10^{-26} \cdot n \cdot 3 \cdot 10^{10} = 1.2 \cdot 10^{-15} \cdot n \quad [\text{s}^{-1}] \quad (8.50)$$

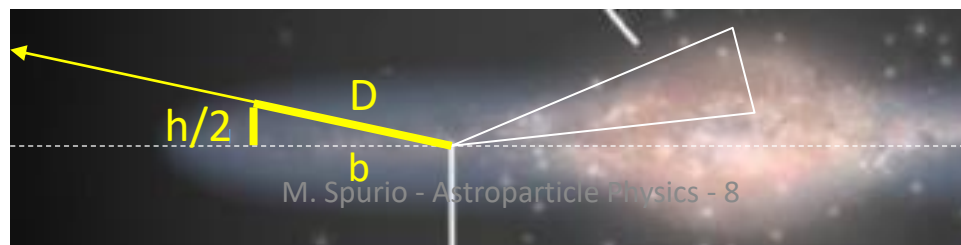
- The cross-section is independent from the CR energy E: the γ -rays emitted isotropically per unit of solid angle $\Delta\Omega$ per cubic centimeter per second corresponds to

$$L_{\gamma}^{\text{diff}} = \frac{\Delta E}{E} \cdot \frac{1}{4\pi} \cdot R_{\text{coll}} \cdot \rho_{CR \rightarrow \gamma} \quad \text{units: } [\text{sr}]^{-1} [\text{s}]^{-1} [\text{eV cm}^{-3}]$$

$$\begin{aligned} L_{\gamma}^{\text{diff}} &= \frac{1}{6} \cdot \frac{1}{4\pi} \cdot (1.2 \cdot 10^{-15}) \cdot n \cdot (0.1) \simeq 10^{-18} \cdot n \quad \text{eV cm}^{-3} \text{ s}^{-1} \text{ sr}^{-1} \\ &= 10^{-24} \cdot n \quad \text{MeV cm}^{-3} \text{ s}^{-1} \text{ sr}^{-1}. \end{aligned} \quad (8.52)$$

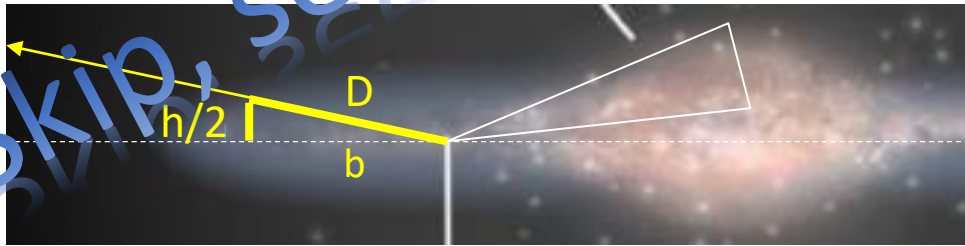
- The quantity in ordinate of [Figure](#) is the spectral energy distribution per unit solid angle, SED/ $\Delta\Omega$. It depends on the linear distance D from which γ -rays from pp interactions can arrive from the galactic plane:

$$\frac{SED}{\Delta\Omega} = L_{\gamma}^{\text{diff}} \cdot D = 10^{-24} \cdot (nD) \quad \text{MeV cm}^{-2} \text{ s}^{-1} \text{ sr}^{-1} \quad (8.53)$$



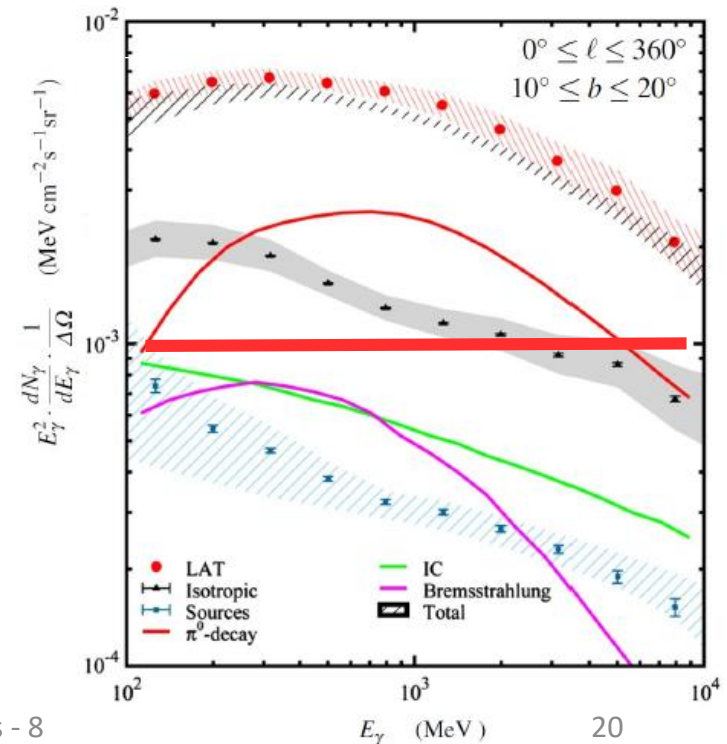
Diffuse flux: a simple estimate

- The observations in Figure refer to $10^\circ < b < 20^\circ$. To estimate D , we use $b = 15^\circ$, and position of the Sun (in a plane in the center of the Galactic disk of $h = 200$ pc).
- Thus, an estimate is $D = (h/2)/\sin 15^\circ = 400$ pc = $1.2 \cdot 10^{21}$ cm.
- The quantity (nD) in (8.53), represents the column density of material responsible for the photons seen by LAT. Our estimate gives $(nD) \sim 10^{21}$ cm $^{-2}$, for $n \sim 1$ cm $^{-3}$.



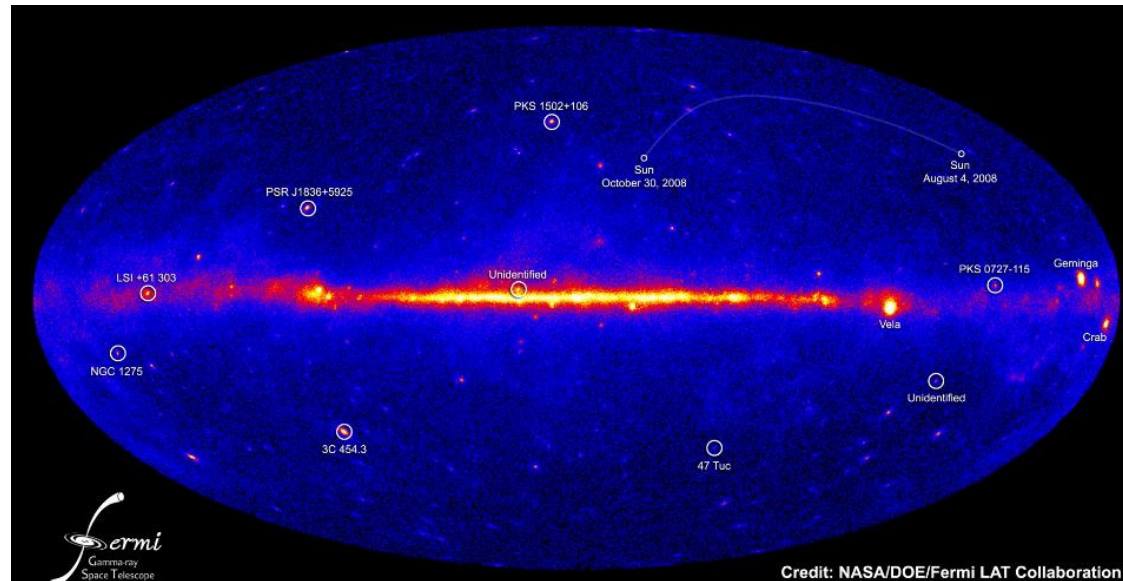
$$\frac{SED}{\Delta\Omega} \simeq 10^{-24} \times 10^{21} = 10^{-3} \text{ MeV cm}^{-2} \text{ s}^{-1} \text{ sr}^{-1}$$

This diffuse γ -ray component is the most direct evidence that CRs are filling our Galaxy with an energy density the same as that measured on Earth.



The sources: The Fermi-LAT Catalogs

- After diffuse flux subtraction, different source catalogs are continuously produced.
- The following information are from the 3rd catalog of HE γ -ray sources (**3FGL**).
- The 3FGL catalog includes **3033** sources within the 100MeV–300 GeV range, with **source location regions, spectral properties, and monthly light curves** for each. Among them:
 - 238 sources are identified based on angular extent or correlated variability (periodic or otherwise) observed at other wavelengths.
 - Pulsars represent the largest Galactic source class
 - 1,100 identified or associated sources are AGN of the blazar class (see Chap. 9)
 - For 1,010 sources, no plausible counterparts at other wavelengths are found.

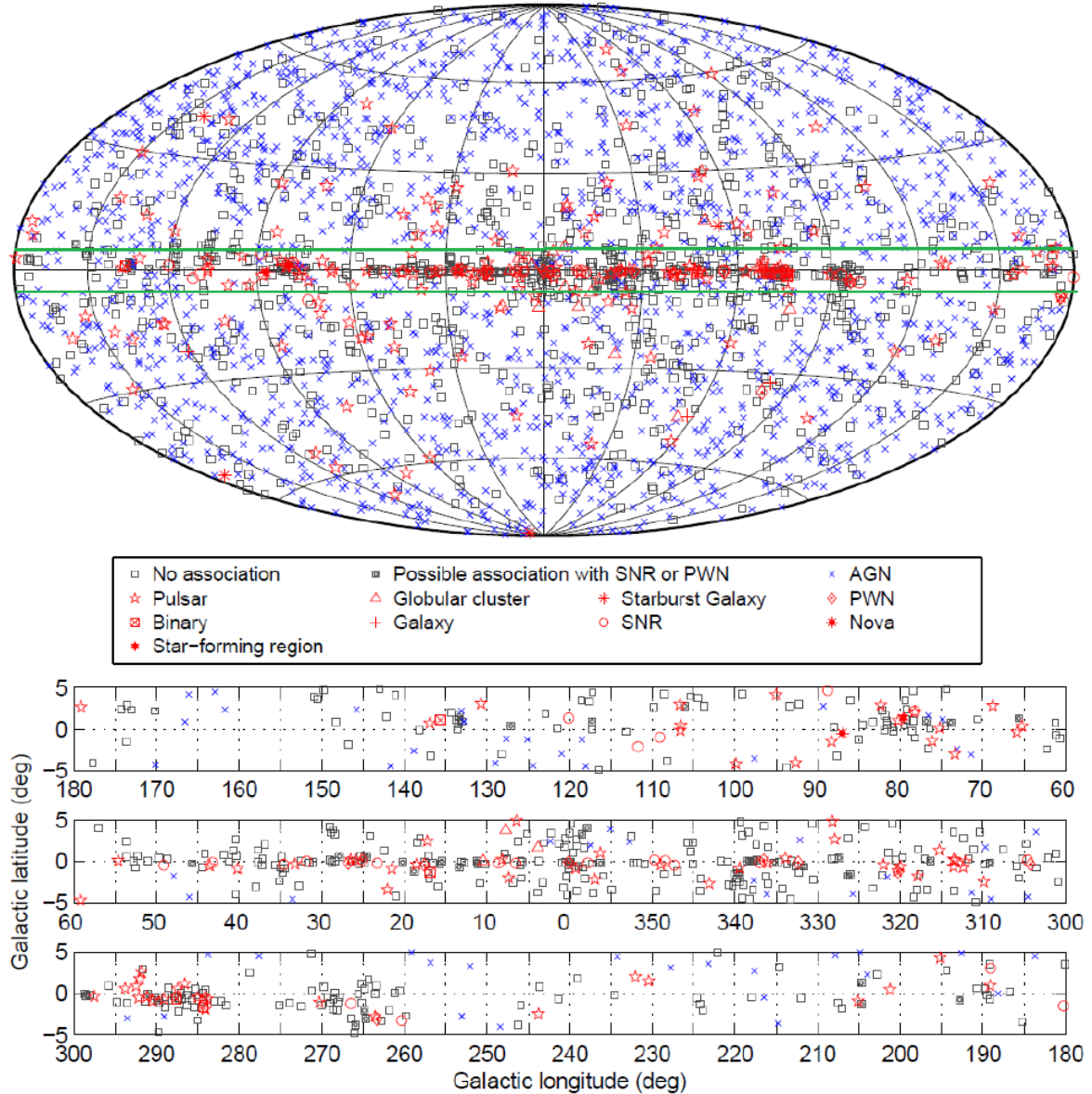


(In Dec 2020, the 4FGL was released, with **5064** objects https://fermi.gsfc.nasa.gov/ssc/data/access/lat/10yr_catalog/)

Gamma-ray Sources in Galactic Coordinates

Fermi-LAT Third
Source Catalog (4y)
arXiv:1501.02003

- Full sky map (top) and blow-up of the inner galactic region (bottom) showing sources by source class (refers to [Table](#)).
- Identified sources are shown with a red symbol, associated in blue.
- All AGN classes are plotted with the same symbol for simplicity

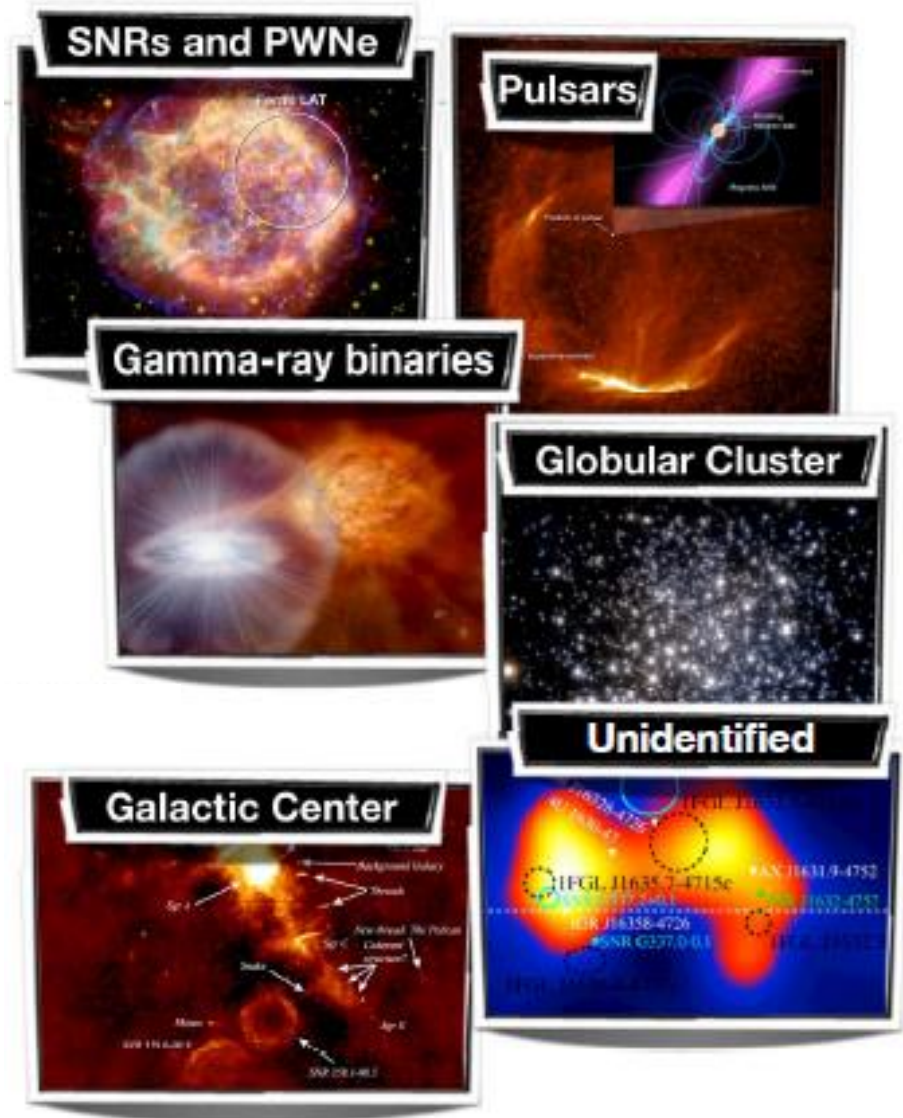


- *Number of objects catalogued in the 3FGL. The first section refers to galactic objects; the second to extragalactic sources.*
- *Identified (associated) objects are indicated with capital (lower case) designators. In the case of AGN, many of the associations have high confidence*

Description	Designator	Identified	Associated
Pulsar, identified by pulsations	PSR	143	-
Pulsar, no pulsations seen in LAT yet	-	-	24
Pulsar wind nebula	PWN	9	2
Supernova remnant	SNR	12	11
Supernova remnant/Pulsar wind nebula	spp	-	49
Globular cluster	GLC	0	15
High-mass binary	HMB	3	0
Binary	BIN	1	0
Nova	NOV	1	0
Star-forming region	SFR	1	0
BL Lac type of blazar	BLL	18	642
FSRQ type of blazar	FSRQ	38	446
Blazar candidate of uncertain type	BCU	5	568
Non-blazar active galaxy	AGN	0	3
Radio galaxy	RDG	3	12
Seyfert galaxy	SEY	0	1
Normal galaxy (or part)	GAL	2	1
Starburst galaxy	SBG	0	4
Narrow line Seyfert 1	NLSY1	2	3
Soft spectrum radio quasar	SSRQ	0	3
Compact Steep Spectrum Quasar	CSS	0	1
Total		238	1785
Unassociated			1010

Classes of galactic sources

- Supernova remnants
- Pulsar wind nebulae
- Pulsars (mostly at GeV energies, few (as the Crab) at $E > 100$ GeV)
- Gamma-ray binaries
- Globular clusters (also at TeV energies?)
- The Galactic center
- Unidentified sources



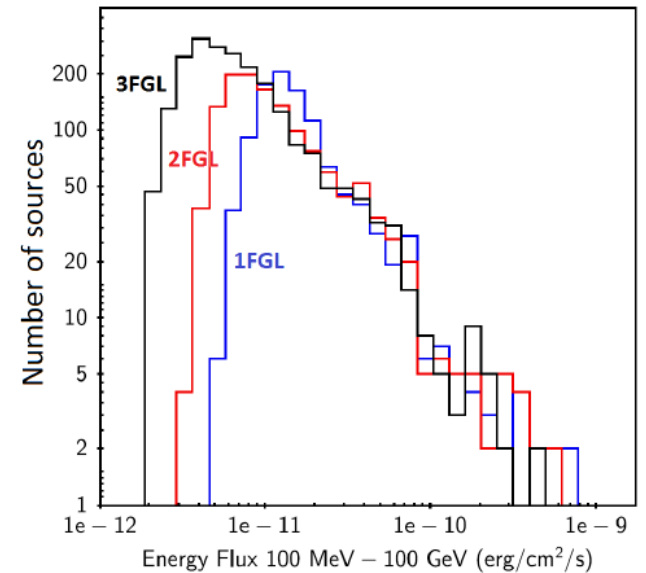
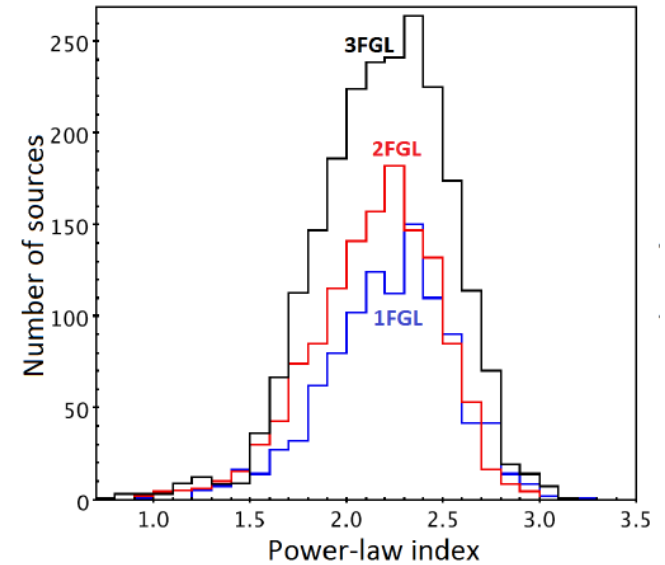
Energy spectral index of LAT sources



- LAT measures the number of arriving γ -ray vs. E_γ ; thus, the flux as a function of E_γ can be constructed for each individual source.
- In most cases, a simple **power law** fits data.

$$\frac{dN}{dE} = K \left(\frac{E}{E_0} \right)^{-\alpha_\gamma} \exp \left(- \frac{E - E_0}{E_c} \right)^b$$

- Frequently, the flux shows a cut-off at high energy and the spectral shape is represented by **exponentially cut-off** power law.
- **Figure: Top:** distribution of the **power-law index** of all of the sources. Its average value is $\alpha_\gamma = 2.19 \pm 0.01$, which is close to that expected for a Fermi mechanism for the acceleration of parent charged particles, $\alpha_{CR} = 2..$
- **Bottom:** Energy flux distribution of detected sources.
- In both cases, high galactic latitudes ($|b| > 10^\circ$) are considered, so most Galactic sources are excluded.
- The red and blue histo refer to older versions of the catalog.

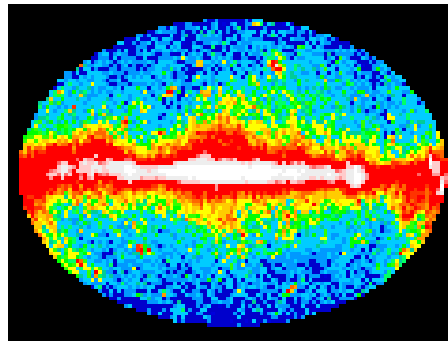


Limits of γ -ray Observations from Space

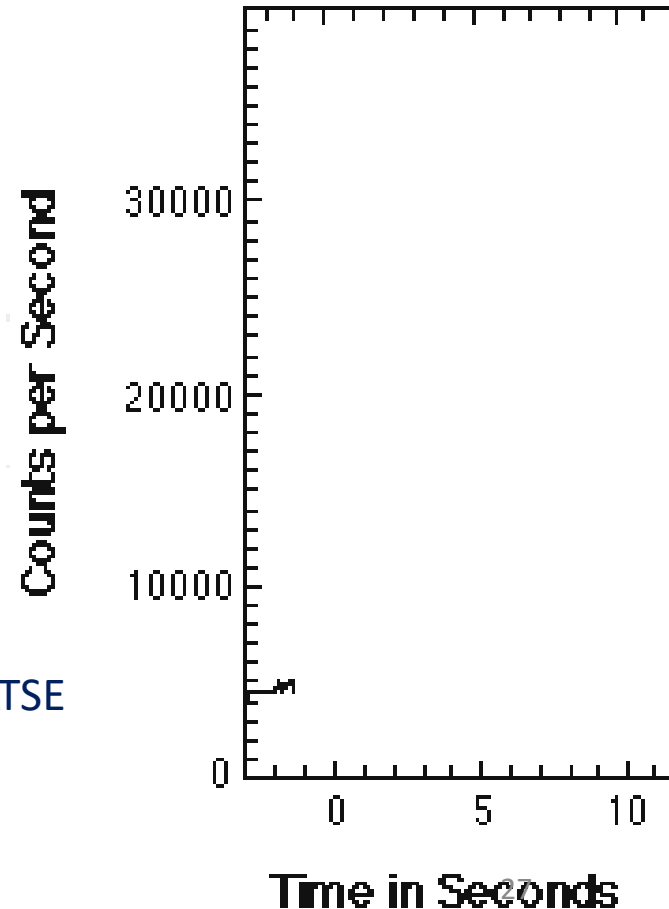
- The limits to the performance of satellite-borne instruments is due to the decreasing photon flux at increasing energies.
- Due to the constraints on the maximum size and weight of an instrument that can be delivered into space, the effective detection area of any satellite experiments is limited to the order of a few m^2 .
- Measuring a flux of photons at TeV energies is almost “impossible” on space
- Instruments with an effective area smaller than 100 m^2 cannot detect the expected astrophysical flux in the TeV energy region. Even with new launch vehicles, a space telescope with an area significantly larger than 10 m^2 is highly uncertain.
- Thus, the next Chapter presents the observation of TeV γ -rays with ground-based experiments.

Transient sources: Gamma Ray Bursts

- Gamma-Ray Bursts (**GRBs**) are extremely intense and relatively short bursts of gamma radiation that occur a few times per day in the detectable Universe.
- Their emission exceeds the γ emission of any other source.
- GRBs occur in random directions in the sky and at cosmological distances.
- The time integrated fluxes, or the fluencies, range from 10^{-7} to 10^{-4} erg cm $^{-2}$ ([cfr](#)).
- The observed fluencies, combined with the distances determined from detections of the host galaxies, show that GRBs are the brightest explosions in the Universe.
- If isotropic, the γ -ray energy output would amount on average to a solar rest-mass energy, $Mc^2 = 10^{54}$ erg, emitted in a few seconds.

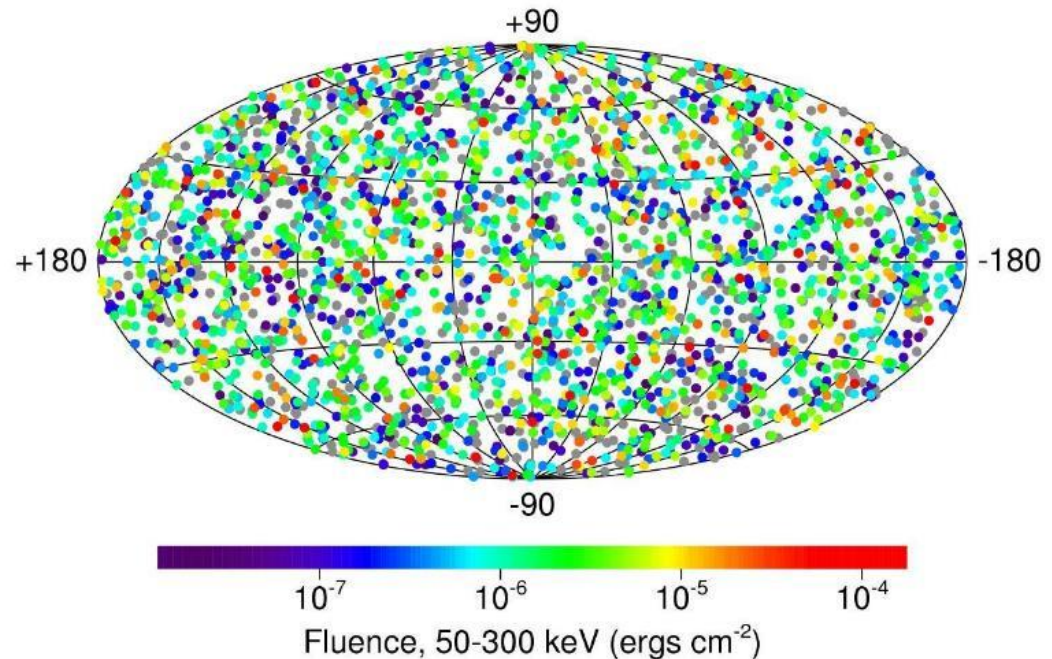


A GRB observed by the BATSE detector on the CGRO



History of GRBs

- Until recently, GRBs were the biggest mystery in HE astronomy.
- They were discovered serendipitously in late 1960s by U.S. military satellites looking for Soviet nuclear testing in violation of the atmospheric nuclear test ban treaty. These satellites carried γ -ray detectors since a nuclear explosion produces γ -rays.
- Only in 1973 the observations were published, identifying a cosmic origin for the previously unexplained observations of γ -rays.
- Another milestone was the [BATSE experiment on the CGRO](#). The main result of BATSE is the conclusive **proof that GRBs occur isotropically** in the sky.
- Thanks to the BATSE data, it has also been possible to measure the typical fluence (the flux integrated over time) of GRBs.



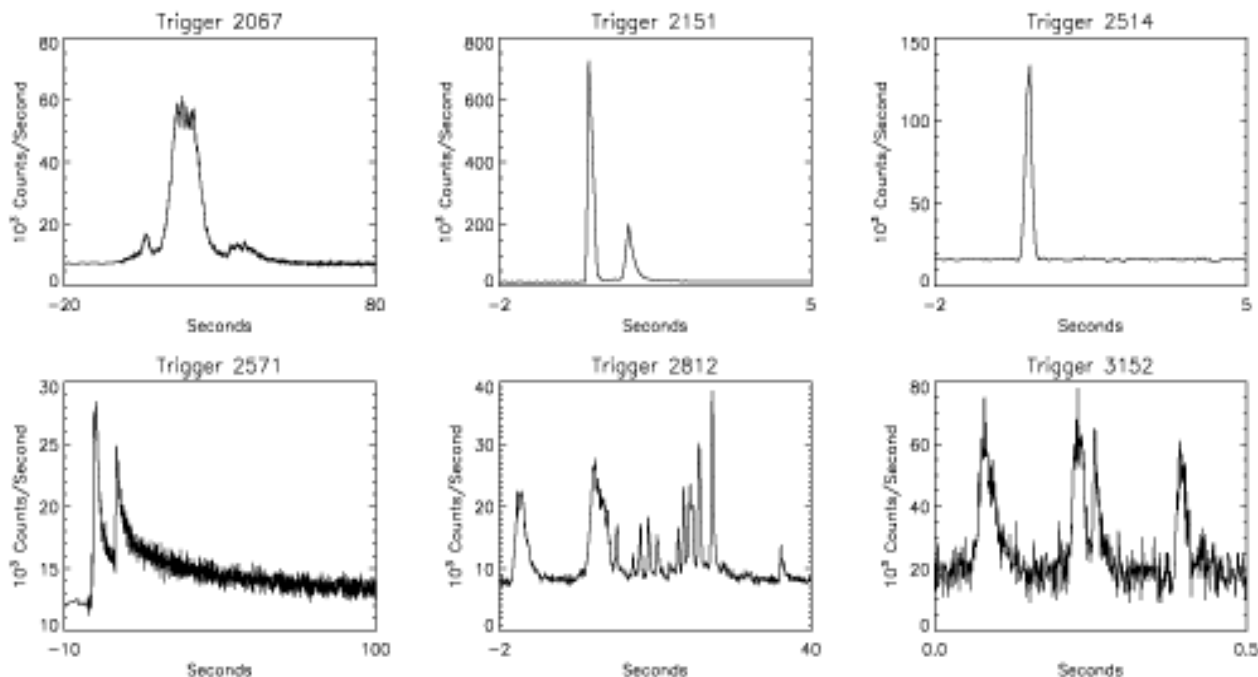
The isotropy of the GRB distribution is evident in this figure. The projection is in galactic coordinates; the plane of the Milky Way Galaxy is along the horizontal line at the middle

Transient: the GRB case

- In astronomy, many transient sources generally have rather simple time structures which help to understand the underlying physics of the objects.
- GRBs are peculiar, as their light curves vary significantly one to another (the **duration**, the **number of peaks**, the **maximum brightness**,...). There are no two identical GRBs.
- BATSE detector catalogued 2,704 GRBs during nine year lifetime (1991 - 2000). It was not equipped to make **afterglow** (see later!) observations.

A sampling of the large variety of GRB time profiles, as detected from BATSE on the the CGRO satellite.

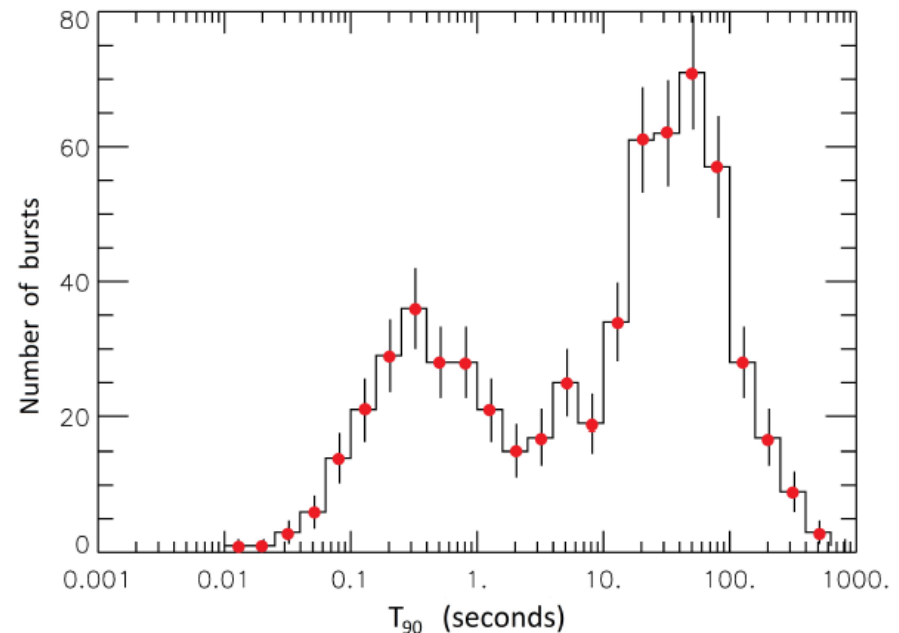
Notice the different time scale on the x-axis



Two types: Long and short GRBs



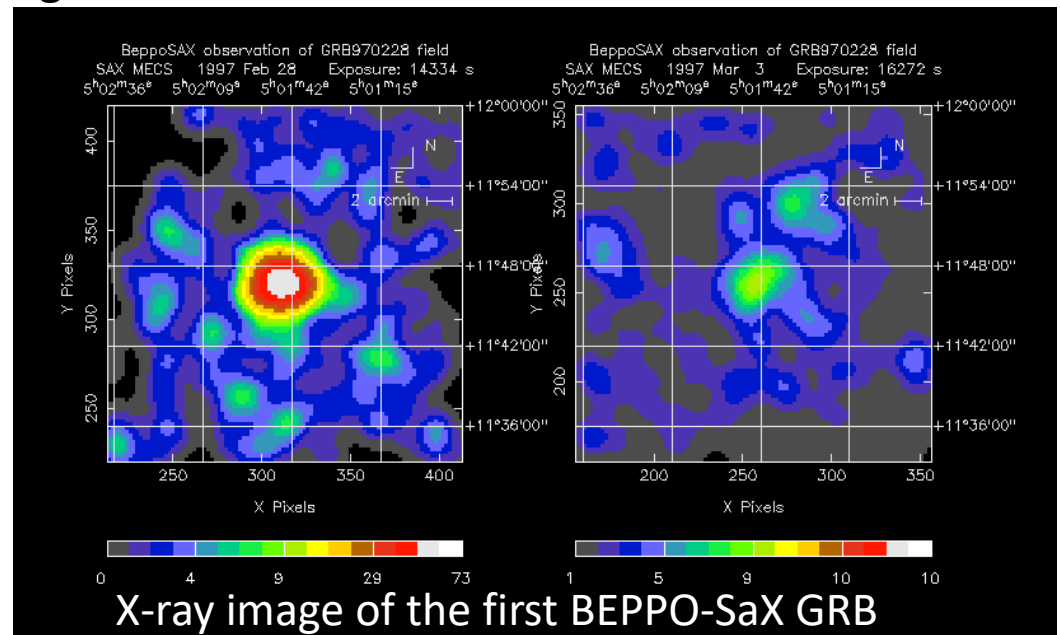
- Observations from BATSE led to the separation of γ -ray bursts into two families
- The main classification is “**long GRBs**” and “**short GRBs**”
 - the long population has an average duration of about 30 s,
 - the short lasts, on average, 0.3 seconds.
 - The conventional separation between the two families is $T_{90}=2$ s
- It has been noticed that the short bursts spectrum is significantly **harder** (with more high energy photons) than the long bursts.
- Long GRBs are the most frequently observed and, therefore, also the best understood.
- **Each family of GRBs is associated with a different progenitor**



Distribution of GRBs that occurred in 2008–2009 as a function of the log of the T_{90} (s). Usually, the duration of the GRB is expressed as the time during which 90% of the counts are detected, and denoted as T_{90} . “Long GRBs” last more than two seconds, the remaining ones are “short GRBs”

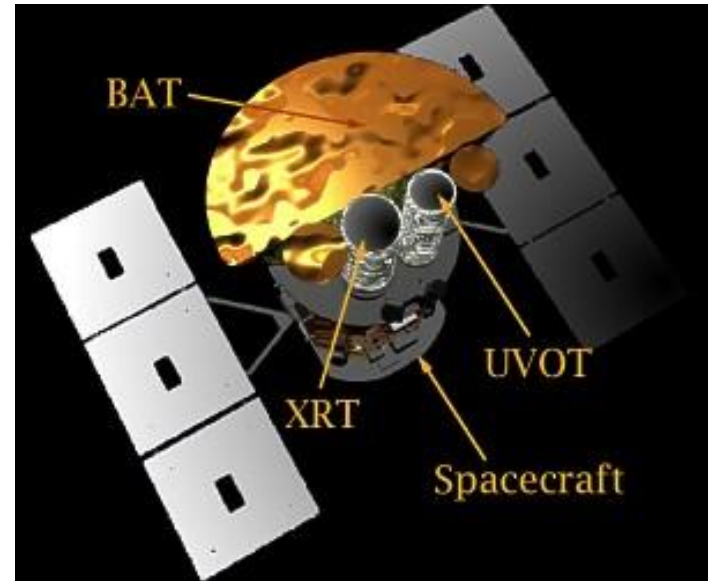
The (Italian) BeppoSAX satellite

- Due to their short duration, GRBs were very difficult to localize precisely.
- In this respect, the real breakthrough was made by the Italian-Dutch satellite BeppoSAX (launch: April 1996). Its Wide Field Camera (WFC), sensitive to the X-ray between 2–25 keV, allowed for measuring the position of the GRBs with uncertainties of only a few arcminutes.
- The satellite could then observe the pinpointed region with the Narrow Field Instrument, covering the 0.1–10 keV range. It was then possible to detect a newly discovered feature: the **X-ray afterglow of the GRB**.
- A Network (the [GCN system](#)) that transmits GRB alerts to a network of selected instruments was set.
- The combination of BeppoSAX WFC trigger and the GCN allowed for all ground-based telescopes to point in the GRB direction to observe optical, IR and radio afterglows.



The SWIFT satellite and others

- Optical observations after the GRB were extremely important to show that long GRBs came from not very bright galaxies, and never very far from the center of its host galaxy.
- This information is useful for inferring that long GRBs are generally associated with massive and short-lived progenitors.
- The **Swift** satellite succeeded BeppoSAX, and contained three instruments: the Burst Alert Detector (BAT), that can turn toward the burst in <100 s the higher angular resolution X-ray (XRT) and UV-optical detectors (UVOT).
- The latest milestone was the launch of the **Fermi**, that hosts (in addition to **LAT**) also the **GBM**.
- Today, the Gamma-ray Coordinates Network (GCN) provides the distribution of GRB and other transient locations detected by various spacecraft, and receives and automatically distributes to the GRB/transients messages about follow-up observations.
- In addition to the LAT and GBM detectors on the Fermi satellite, and the instruments on the Swift, AGILE, and INTEGRAL satellites, there were others satellites in the past that were able to observe GRBs, and others are planned for the future



Progenitors of GRBs

- **Long GRBs.** Long GRBs occur mostly in star-forming galaxies. In several cases, long GRBs are correlated with supernovae, linking them to the death of massive stars (Chap. 12).
- The connection between supernovae and longGRBs is given by the total emitted kinetic energy, unambiguously observed with **GRB 980425** in conjunction with SN 1998bw.
- These two events were coincident both in time and space, and the energetic coincidence left few doubts about the connection with the *hypernova* model, §12.13.3.
- **Short GRBs.** Short GRBs are rarer. Models on the origin of short GRBs had to wait for the detection of a large sample of afterglows by Swift.
- Afterglows allowed for the identification of sGRBs host galaxies: sGRBs occur within galaxies that contain a considerable quantity of **old stars**.
- The energy emitted by short GRBs exceeds that of long GRBs by orders of magnitude.
- The current hypothesis attributes the origin of short GRBs to the **merging of two compact objects**, as two neutron stars or neutron star-black hole.
- Such structures lose energy due to gravitational radiation and the two objects will spiral closer and closer. This process is thought to be extremely fast (no more than a few seconds), in agreement with the observation of short GRBs.
- **This mechanism was spectacularly confirmed in the occurrence of GRB170817A, also detected in coincidence with a GW, Chapter 13.**

Model of GRBs: the fireball

- The **fireball model** predicts that γ -rays and afterglow must arise from an emission region moving at relativistic velocities, likely independent of the progenitor.
- The energy release in such compact regions produces a luminosity that exceeds the Eddington luminosity, above which radiation pressure overwhelms gravity.
- The inner engine is attributed to a compact object, the hypernova or the merger of two compact objects. This inner engine causes an explosion that originates the relativistic blast waves moving at relativistic speeds (the fireball).
- Two opposite jets form along the rotation axis of the accretion disk
- During the acceleration in the jets, newly formed material accelerates faster and forms consecutive shells with different speeds.
- Interactions of shells with the external medium or collisions between shells reconvert the kinetic energy into internal energy, radiated as γ -rays.
- Shocks between shells are responsible for the emission of γ -rays

